Regulatory mechanism of length-dependent activation in skinned porcine ventricular muscle: role of thin filament cooperative activation in the Frank-Starling relation

Takako Terui,[1] Yuta Shimamoto,[2] Mitsunori Yamane,[2] Fuyu Kobirumaki,[1] Iwao Ohtsuki,[1] Shin'ichi Ishiwata,[2] Satoshi Kurihara,[1] and Norio Fukuda[1]

[1]Department of Cell Physiology, The Jikei University School of Medicine, Tokyo 105-8461, Japan
[2]Department of Physics, Waseda University, Tokyo 169-8555, Japan

Cardiac sarcomeres produce greater active force in response to stretch, forming the basis of the Frank-Starling mechanism of the heart. The purpose of this study was to provide the systematic understanding of length-dependent activation by investigating experimentally and mathematically how the thin filament "on–off" switching mechanism is involved in its regulation. Porcine left ventricular muscles were skinned, and force measurements were performed at short (1.9 µm) and long (2.3 µm) sarcomere lengths. We found that 3 mM MgADP increased Ca^{2+} sensitivity of force and the rate of rise of active force, consistent with the increase in thin filament cooperative activation. MgADP attenuated length-dependent activation with and without thin filament reconstitution with the fast skeletal troponin complex (sTn). Conversely, 20 mM of inorganic phosphate (Pi) decreased Ca^{2+} sensitivity of force and the rate of rise of active force, consistent with the decrease in thin filament cooperative activation. Pi enhanced length-dependent activation with and without sTn reconstitution. Linear regression analysis revealed that the magnitude of length-dependent activation was inversely correlated with the rate of rise of active force. These results were quantitatively simulated by a model that incorporates the Ca^{2+}-dependent on–off switching of the thin filament state and interfilament lattice spacing modulation. Our model analysis revealed that the cooperativity of the thin filament on–off switching, but not the Ca^{2+}-binding ability, determines the magnitude of the Frank-Starling effect. These findings demonstrate that the Frank-Starling relation is strongly influenced by thin filament cooperative activation.

INTRODUCTION

At the turn of the 20th century, Frank and Starling discovered that cardiac pump function is enhanced as ventricular filling is increased (i.e., the Frank-Starling law of the heart; see Katz, 2002 and references therein). The "law" forms the fundamental principle of the heart in cardiovascular physiology, defining the relation between the diastolic and systolic performances of cardiac chambers. It is widely accepted that the length dependence of Ca^{2+}-based myofibrillar activation (i.e., expressed as "Ca^{2+} sensitivity of force") largely underlies the law (e.g., Allen and Kurihara, 1982; Allen and Kentish, 1985; Kentish et al., 1986); however, the molecular mechanism of this seemingly simple phenomenon still remains elusive and warrants an in-depth investigation.

The cross-bridge formation is a stochastic process in the striated muscle sarcomere (e.g., Huxley, 1957).

Therefore, it has been proposed that the binding of myosin to actin is enhanced upon the reduction in the distance between the thick and thin filaments (i.e., interfilament lattice spacing), resulting in an increase in active force production and, apparently, Ca^{2+} sensitivity of force (Ishiwata and Oosawa, 1974; McDonald and Moss, 1995; Fuchs and Wang, 1996; Fukuda et al., 2000). Indeed, studies with synchrotron x ray revealed that passive force due to extension of the giant elastic protein titin (also known as connectin) modulates the lattice spacing within the physiological sarcomere length (SL) range in cardiac muscle (Cazorla et al., 2001; Fukuda et al., 2003, 2005). Konhilas et al. (2002b), however, challenged this proposal, demonstrating that the lattice spacing and Ca^{2+} sensitivity of force are not well correlated. Therefore, factors other than the titin-based lattice spacing modulation are likely at play in the regulation of length-dependent activation.

As has been reported, multiple cooperative processes are involved in active force generation in striated muscle

---

T. Terui and Y. Shimamoto contributed equally to this paper.

Correspondence to Norio Fukuda: noriof@jikei.ac.jp

Y. Shimamoto's present address is Laboratory of Chemistry and Cell Biology, The Rockefeller University, 1230 York Avenue, New York, NY 10065.

Abbreviations used in this paper: NEM-S1, N-ethylmaleimide myosin subfragment 1; n_H, Hill coefficient; Pi, inorganic phosphate; PLV, porcine left ventricular muscle; SL, sarcomere length; sTn, fast skeletal troponin complex; Tn, troponin.

(e.g., Brandt et al., 1982, 1987, 1990; Moss et al., 1985); i.e., cooperative binding of Ca^{2+} to troponin (Tn) C (TnC), cooperative binding of myosin to the thin filaments, and synergistic interactions between myosin binding to actin and Ca^{2+} binding to TnC (e.g., Bremel et al., 1973; Güth and Potter, 1987; Hoar et al., 1987; Zot and Potter, 1989; Swartz and Moss, 1992). Likewise, it is widely accepted that the formation of strongly bound cross-bridges enhances cooperative recruitment of neighboring myosin to the thin filaments. Bremel and Weber (1972) were the first to demonstrate in solution that an increase in the fraction of rigor cross-bridges (rigor myosin subfragment 1) cooperatively activates myosin ATPase, as with the increased Ca^{2+} concentration, indicating that Ca^{2+} and strongly bound cross-bridges synergistically regulate the "on–off" equilibrium of the thin filament state. Later, the group of Moss provided evidence in skinned muscle fibers that actomyosin interaction is indeed promoted in the presence of the strong-binding cross-bridge analogue *N*-ethylmaleimide myosin subfragment 1 (NEM-S1) via activation of the thin filaments, as manifested by the increased rate of contraction (Swartz and Moss, 1992, 2001; Fitzsimons et al., 2001a,b) and the increased Ca^{2+} sensitivity of force (Fitzsimons and Moss, 1998; Fitzsimons et al., 2001a,b). Similarly, we previously reported that the application of MgADP, i.e., the ensuing formation of the actomyosin–ADP complex, cooperatively enhances cross-bridge recruitment and that of inorganic phosphate (Pi) does the opposite in skinned fibers of cardiac and skeletal muscles (Shimizu et al., 1992; Fukuda et al., 1998, 2000, 2001a).

Earlier studies have suggested that the thin filament–based on–off switching mechanism is involved in the regulation of length-dependent activation in cardiac muscle. Indeed, Fitzsimons and Moss (1998) reported that length-dependent activation is attenuated in the presence of NEM-S1. Fukuda et al. (2000) confirmed this notion by providing evidence that the length dependence becomes smaller in the presence of MgADP (hence the actomyosin–ADP complex). It has also been reported that direct modulation of thin filament regulatory proteins, e.g., Tn isoform changes (Arteaga et al., 2000; Terui et al., 2008) or TnI point mutation (Tachampa et al., 2007), markedly affects length-dependent activation. Therefore, it is likely that length-dependent activation depends on the state of the thin filaments, either modulated directly by regulatory protein isoform switching or indirectly by strongly bound cross-bridges. However, it is still unknown how Ca^{2+}-dependent on–off switching of the thin filament state and interfilament lattice spacing coordinate to regulate myocardial length-dependent activation.

Accordingly, this study was undertaken to systematically uncover the molecular basis of length-dependent activation in cardiac muscle, focusing on the role of thin filament cooperative activation. We varied the level of thin filament cooperative activation in skinned porcine left ventricular muscle (PLV) directly by Tn exchange or indirectly by the application of MgADP or Pi, or the combination of both. Our analysis revealed that the magnitude of length-dependent activation is inversely related to the rate of rise of active force, highlighting a pivotal role of thin filament cooperative activation in the regulation of the Frank-Starling relation. Furthermore, our mathematical model analyses revealed the relationship between the characteristics of thin filament activation and length-dependent activation, and led us to conclude that length-dependent activation is under the strong control of thin filament cooperative activation.

MATERIALS AND METHODS

All experiments performed in this study conform to the Guide for the Care and Use of Laboratory Animals (1996. National Academy of Sciences, Washington D.C.). For expanded materials and methods, please see the supplemental material.

Preparation of skinned muscle
Skinned muscles were prepared according to the method in our recent studies (Terui et al., 2008; Matsuba et al., 2009). In brief, porcine hearts (from ~1.0-yr-old animals) were obtained from a local slaughterhouse. Muscle strips (1–2 mm in diameter and ~10 mm in length) were dissected from the papillary muscle of the left ventricle in Ca^{2+}-free Tyrode's solution (see Fukuda et al., 2001a for composition) containing 30 mM 2,3-butanedione monoxime (BDM).

Muscle mechanics
Isometric force was measured according to the method in our recent studies (Terui et al., 2008; Udaka et al., 2008; Matsuba et al., 2009). In brief, PLVs were skinned in relaxing solution (5 mM MgATP, 40 mM BES, 1 mM Mg^{2+}, 10 mM EGTA, 1 mM dithiothreitol, 15 mM phosphocreatine, 15 U/ml creatine phosphokinase (CPK), and 180 mM ionic strength [adjusted by K-propionate], pH 7.0), containing 1% (wt/vol) Triton X-100 and 10 mM BDM overnight at ~3°C (Fukuda et al., 2003, 2005). Muscles were stored for up to 3 wk at −20°C in relaxing solution containing 50% (vol/vol) glycerol. All solutions contained protease inhibitors (0.5 mM PMSF, 0.04 mM leupeptin, and 0.01 mM E64).

Small thin preparations (~100 µm in diameter and ~2 mm in length) were dissected from the porcine ventricular strips for force measurement. SL was measured by laser diffraction during relaxation, and active and passive forces were measured at 15°C (pCa adjusted by Ca^{2+}/EGTA based on a computer program by Fabiato, 1988). MgADP (up to 10 mM) or Pi (up to 20 mM) was added to the individual activating solutions in accordance with our previous studies (Fukuda et al., 2000, 2001a), while maintaining ionic strength at 180 mM. When MgADP was present, 0.1 mM P^1,P^5-di(adenosine-5′)pentaphosphate was added to both activating and relaxing solutions, with no CPK to maintain the ADP/ATP ratio (Fukuda et al., 1998, 2000). We also used pimobendan (provided by Nippon Boehringer Ingelheim) to increase the affinity of TnC for Ca^{2+} (Fukuda et al., 2000). Pimobendan was initially dissolved in DMSO and diluted with the individual solutions (Fukuda et al., 2000). The final concentration of DMSO was 1%, having no effect on active or passive force, as observed in our previous study (Fukuda et al., 2000).

The muscle preparation was first immersed in relaxing solution, and SL was set at 1.9 µm. Active and passive forces were measured at 1.9 µm and then at 2.3 µm, as described in our previous studies (rundown <10% for active and passive forces; Fukuda et al., 2003, 2005; Terui et al., 2008). Active force data were fitted to the Hill equation (Fukuda et al., 2000), and the difference between the values of the midpoint of the force–pCa curve (i.e., pCa_{50}) at SL 1.9 and 2.3 µm was used as an index of the SL dependence of Ca^{2+} sensitivity of force (expressed as ΔpCa_{50}). The steepness of the force–pCa curve was expressed as the Hill coefficient (n_H).

The rate of rise of active force was assessed according to the method in our previous work (Fukuda et al., 2001b), using the preparations used for the steady-state isometric force measurement. In brief, SL was set at 1.9 µm in relaxing solution. The preparation was then immersed in low EGTA (0.5 mM) relaxing solution for 1 min and transferred to the control activating solution (5 mM MgATP, 40 mM BES, 1 mM Mg^{2+}, 10 mM EGTA, 1 mM dithiothreitol, 15 mM phosphocreatine, 15 U/ml CPK, and 180 mM ionic strength (adjusted by K-propionate), pH 7.0, pCa 4.5), without MgADP or Pi, followed by relaxation. The procedure was then repeated in the presence of MgADP or Pi (or after Tn reconstitution), and the time to half-maximal activation was compared with that obtained in the preceding contraction in the same preparation, hence minimizing the effect of diffusion that is dependent on the muscle thickness. The ratio of the time to half-maximal activation, defined as $t_{1/2}$, was used as an index of cooperativity of cross-bridge recruitment.

In some experiments, the velocity of isometric force development was obtained at half-maximal activation in the presence of MgADP (up to 10 mM) or Pi (up to 20 mM), and the value was compared with that in the preceding contraction in the same preparation with no MgADP or Pi (pCa 4.5 and SL, 1.9 µm). The ratio of the velocity of isometric force development was defined as $V_{1/2}$.

Tn exchange

The fast skeletal Tn complex (sTn) was extracted from rabbit fast skeletal muscle, and Tn exchange (2 mg/ml for 1 h) was performed on PLV, according to our previously published procedure (see Terui et al., 2008; Matsuba et al., 2009). As detailed in these previous reports, our protocol allowed for only a small increase (∼10%) in the band intensity of each Tn subunit upon sTn reconstitution.

Control experiments showed that the treatment of PLV with the Tn complex (6 mg/ml for 1 h under the same condition) from the porcine ventricle does not alter the steady-state active force or $t_{1/2}$ at various Ca^{2+} concentrations (see Matsuba et al., 2009; not depicted). Also, due to a relatively greater magnitude of rundown in steady-state active force (i.e., ∼30%; not depicted), we did not conduct mechanical experiments in the present study using PLV that had been incorporated with the cardiac Tn complex after sTn reconstitution.

Model analysis

The model calculates the active isometric force at a given SL and at a given Ca^{2+} concentration, based on the SL-dependent change in the lattice spacing and the Ca^{2+}-based on–off switching of the thin filament state. The on–off state was defined according to the lateral fluctuation of the thin filaments in the myofilament lattice (Ishiwata and Fujime, 1972; Umazume and Fujime, 1975; Yoshino et al., 1978; Yanagida et al., 1984; see Fig. S1); however, the lateral fluctuation does not necessarily represent the physical thermal fluctuation of the thin filaments, but rather, it mathematically portrays the equilibrium of the thin filament state between "off" and "on," depending on the Ca^{2+} concentration (Solaro and Rarick, 1998).

In our model, the overlap length between the thick and thin filaments at a SL of L is given by:

$$\frac{1}{2}(L_0 - L), \tag{1}$$

where L_0 (3.8 µm) is the maximal SL at no filament overlap. Thick and thin filament length was assumed to be 1.6 and 1.1 µm, respectively (Sosa et al., 1994). In this study, the overlap length was set to be constant (0.75 µm), independent of SL because in the SL range between 1.9 and 2.3 µm (where the experiments were performed), the number of myosin heads in the overlap region reportedly remains constant based on the thick filament geometry (Sosa et al., 1994).

Next, we assumed that the lattice spacing, d, decreases upon the increase in SL under the constant lattice volume, V, as has been observed in x-ray diffraction studies (Cazorla et al., 2001; Fukuda et al., 2003, 2005), according to the following equation:

$$V = d^2 \cdot L. \tag{2}$$

Based on the value of d_{10} (i.e., the d_{10} lattice spacing) of 43 nm at SL 2.0 µm (see Fukuda et al., 2003 for the d_{10} value of sarcomeres expressing both N2B and N2BA titins at similar levels, as in PLV; Terui et al., 2008), the lattice spacing is estimated to be 28.7 nm, and thereby the lattice volume, V, was set to be 0.0016 µm³.

Next, we described the position-dependent probability of actomyosin interaction by the Gaussian distribution (Ishiwata and Oosawa, 1974):

$$P(q) = \frac{1}{\sqrt{\pi}\sigma_A{}^2} \exp(-q^2 / \sigma_A{}^2), \tag{3}$$

where q is a lateral coordinate perpendicular to the filament long axis, and σ_A is the width of the Gaussian distribution (variance, $\sigma_A{}^2/2$). To take into account the Ca^{2+}-dependent change of the actomyosin interaction, the degree of σ_A was changed in accordance with the Ca^{2+} concentration based on the Hill equation (see Ishiwata and Oosawa, 1974 and Figs. S1 and S2):

$$\sigma_A(pCa) = \sigma_{max} \frac{1}{1 + 10^{-n_{H\_actin}(pCa_{50\_actin} - pCa)}}, \tag{4}$$

where σ_{max} is the maximal width of the Gaussian distribution (21 nm), determining the maximal interaction probability at the saturating Ca^{2+} concentration (pCa 4.5). The parameter n_{H_actin} represents the cooperativity of thin filament activation in the model calculation, and pCa_{50_actin} represents the sensitivity of the thin filaments to Ca^{2+}.

Here, we considered that the actomyosin interaction takes place over the region where the lateral coordinate, q, exceeds a certain distance, $d-a$, because myosin heads are located apart from the thick filament backbone up to a distance a (24 nm). The cumulative interaction probability with respect to the unit overlap length, I, is therefore given by:

$$I = \int_{d-a}^{\infty} P(q)dq. \tag{5}$$

Finally, the active isometric force at a given SL and pCa is expressed as the product of overlap length and interaction probability:

$$F = F_0 \cdot \frac{1}{2}(L_0 - L) \cdot \frac{1}{\sqrt{\pi}} \cdot \frac{1}{\sigma_A(pCa)} \int_{d-a}^{\infty} \exp(-q^2 / \sigma_A{}^2(pCa))dq, \tag{6}$$

where F_0 (45 and 36, for control and sTn-reconstituted PLV, respectively) is the fitting parameter to quantitatively simulate the experimental results.

Statistics
Significant differences were assigned using the paired or unpaired Student's t test as appropriate. Data are expressed as mean ± SEM, with n representing the number of muscles. Linear regression analyses were performed in accordance with the method described in previous studies (Fukuda et al., 2001b; Terui et al., 2008). Statistical significance was assumed to be P < 0.05. NS indicates P > 0.05.

Online supplemental material
The supplemental material provides an expanded description of our model analysis. In addition, Fig. S1 shows a schematic illustration of our model used to simulate the present experimental data. Fig. S2 provides characteristics of our model, showing how Ca^{2+} sensitivity of force is changed in response to a change in thin filament cooperative activation. Fig. S3 shows the relation of Ca^{2+} binding to the thin filaments or thin filament cooperative activation versus length-dependent activation in our model. Fig. S4 shows the experimentally observed effect of MgADP on the rate of active force redevelopment, k_{tr} (overall cross-bridge cycling rate; see Discussion), at varying activation levels. Fig. S5 shows the experimentally obtained relation between SL and active force at

various Ca^{2+} concentrations (converted from force–pCa curves) and the simulation by our model. Fig. S6 shows the model simulation showing the effect of an increase in the average length of myosin heads on Ca^{2+} sensitivity of force and length-dependent activation. The online supplemental material is available at http://www.jgp.org/cgi/content/full/jgp.201010502/DC1.

RESULTS

Effect of MgADP or Pi on the rate of rise of active force
First, we investigated the effect of various concentrations of MgADP or Pi on the rate of rise of active force under the control condition without sTn reconstitution. We found that MgADP significantly decreased $t_{1/2}$ at low concentrations (1 and 3 mM) but increased it at a high concentration (10 mM) (Fig. 1 A), and Pi exerted apparently similar effects at low (1, 3, and 5 mM) and high (10 and 20 mM) concentrations (Fig. 1 B). The accelerating effect of MgADP was maximal at 3 mM, whereas the decelerating effect of Pi reached a quasi-plateau at 10 mM. Therefore, based on the previous studies indicating that the rate of contraction is modulated by a change in the fraction of strongly bound cross-bridges via alteration of the on–off
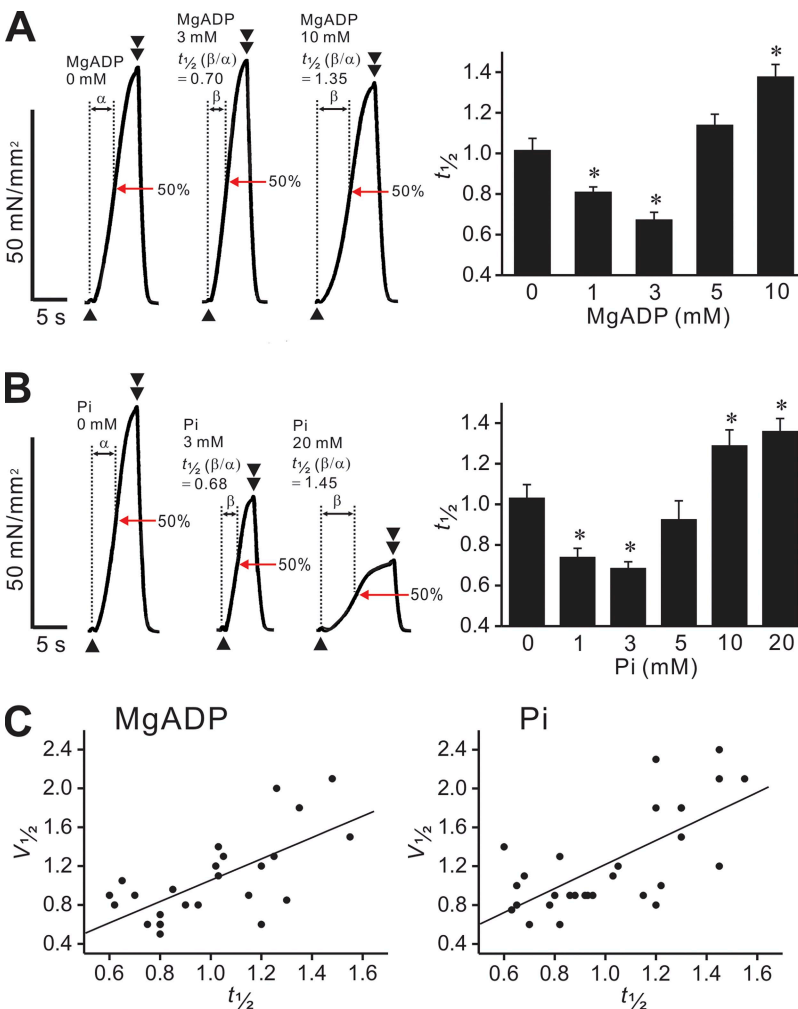

Figure 1. Effect of MgADP or Pi on the rate of rise of active force. pCa 4.5; SL, 1.9 µm. (A) Effect of MgADP. (Left) Typical chart tracings showing active force responses in the absence and presence of 3 and 10 mM MgADP (in the same preparation). (Right) Graph summarizing the effects of various concentrations of MgADP on $t_{1/2}$. *, P < 0.05 compared with 0 mM MgADP. Active force compared with 0 mM MgADP (in percent) was 99.87 ± 3.74, 97.37 ± 5.57, 93.21 ± 5.44, and 90.07 ± 3.27, with 1, 3, 5, and 10 mM MgADP, respectively. n = 5. (B) Effect of Pi. (Left) Typical chart tracings showing active force responses in the absence and presence of 3 and 20 mM Pi (in the same preparation). (Right) Graph summarizing the effects of various concentrations of Pi on $t_{1/2}$. *, P < 0.05 compared with 0 mM Pi. Active force compared with 0 mM MgADP (in percent) was 79.16 ± 2.07, 57.62 ± 3.55, 44.06 ± 2.96, 35.02 ± 3.73, and 28.62 ± 3.31, with 1, 3, 5, 10, and 20 mM Pi, respectively. n = 5. In both A and B, arrowheads and double arrowheads indicate the points at which solution was switched from low EGTA (0.5 mM) relaxation to contraction and from contraction to high EGTA (10 mM) relaxation, respectively. The time to half-maximal activation (50%) was measured as indicated by α and β, and the relative value, i.e., β/α, was obtained for each preparation and defined as $t_{1/2}$. Note that $t_{1/2}$ is ∼1.0 in the absence of MgADP or Pi, indicating reproducibility of the rate of rise of active force. (C) Relation between $t_{1/2}$ and $V_{1/2}$ obtained in the presence of varying concentrations of MgADP (left, 0–10 mM) and Pi (right, 0–20 mM). A significant linear relationship existed for both MgADP (R = 0.68; P < 0.0005) and Pi (R = 0.70; P < 0.0001). Data taken from bar graphs in A and B.
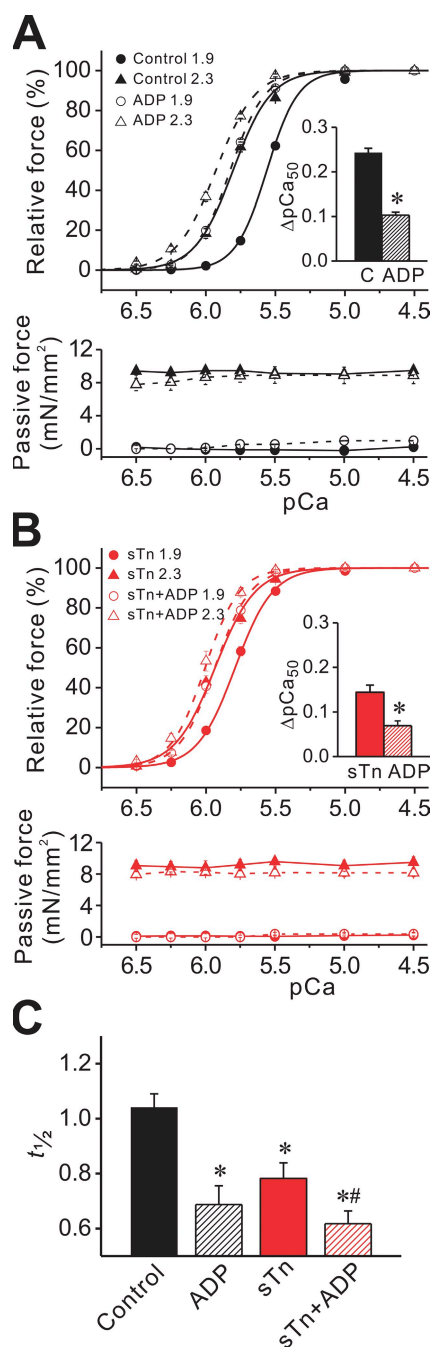
Figure 2. Effects of MgADP on Ca^{2+} sensitivity of force and $t_{1/2}$ with and without sTn reconstitution. (A) Effect of 3 mM MgADP on force–pCa curves (top) and passive force (bottom) in control PLV. Solid lines, −MgADP; dashed lines, +MgADP. (Inset) Comparison of ΔpCa_{50} in the absence and presence of MgADP. "C" indicates control without MgADP. *, $P < 0.05$. (B) Same as in A, but thin filaments were reconstituted with sTn. Solid lines, −MgADP; dashed lines, +MgADP. (Inset) Comparison of ΔpCa_{50} in the absence and presence of MgADP. "sTn" indicates sTn-reconstituted PLV without MgADP. *, $P < 0.05$. (C) Comparison of $t_{1/2}$ in control and sTn-reconstituted muscles in the absence and presence of 3 mM MgADP. *, $P < 0.05$ compared with control; #, $P < 0.05$ compared with sTn. $n = 6$–7.

equilibrium of the thin filament state (Swartz and Moss, 1992, 2001; Fitzsimons et al., 2001a,b), we regarded 3 mM MgADP as the amount to enhance thin filament cooperative activation and 20 mM Pi to reduce it and used them in the following experiments.

Fig. 1 C shows the relationship between $t_{1/2}$ and $V_{1/2}$. We found that a significant linear relationship with a similar slope value existed between the parameters in the presence of varying concentrations of MgADP (Fig. 1 C, left; slope 1.07) or Pi (right, slope 1.24), indicating that $t_{1/2}$ reflects the rate of rise of active force.

Effect of MgADP or Pi on length-dependent activation with and without sTn reconstitution

Next, we investigated how the SL-dependent increase in Ca^{2+} sensitivity of force responds to alteration of thin filament cooperative activation. In this series of experiments, we performed sTn reconstitution to directly enhance thin filament cooperative activation, as demonstrated in our previous study (Terui et al., 2008), with and without MgADP or Pi.

We found that 3 mM MgADP or sTn reconstitution similarly shifted the force–pCa curve leftward, to a greater magnitude at SL 1.9 μm than at 2.3 μm, and consequently decreased ΔpCa_{50} (Fig. 2, A and B). Ca^{2+} sensitivity of force was synergistically increased by MgADP in sTn-reconstituted PLV, accompanied by a marked attenuation of length-dependent activation (Fig. 2 B). As shown in Fig. 2 C, the rate of rise of active force was increased by MgADP or sTn reconstitution by a similar magnitude. Similar to the finding on Ca^{2+} sensitivity of force, the rate of rise of active force was increased by MgADP in sTn-reconstituted PLV (Fig. 2 C).

We then tested the effect of Pi on length-dependent activation. Without sTn reconstitution, 20 mM Pi shifted the force–pCa curve rightward to a greater magnitude at SL 1.9 μm than at 2.3 μm, and consequently increased ΔpCa_{50} (Fig. 3 A). Pi increased ΔpCa_{50} also in sTn-reconstituted PLV (Fig. 3 B). In contrast to MgADP, Pi retarded the rate of rise of active force in both control and sTn-reconstituted PLV (Fig. 3 C). The values of pCa_{50}, n_H, and maximal force at SL 1.9 and 2.3 μm under various conditions are summarized in Table I.

Fig. 4 summarizes the relationship between $t_{1/2}$, pCa_{50} and ΔpCa_{50} obtained with MgADP or Pi in control and sTn-reconstituted PLV. We found that pCa_{50} and ΔpCa_{50} were linearly correlated with each other (Fig. 4 A), and that pCa_{50} and ΔpCa_{50} were a linear function of $t_{1/2}$ (Fig. 4, B and C). As reported previously (Dobesh et al., 2002), however, no significant correlation was found between n_H and pCa_{50} or ΔpCa_{50} (Fig. 5).

Effect of pimobendan on length-dependent activation with and without sTn reconstitution

The observed relationship of Ca^{2+} sensitivity of force and length-dependent activation may be a consequence

associated with the leftward shift of the force–pCa curve (Hanft et al., 2008). We therefore tested the effect of pimobendan on length-dependent activation, with passive force carefully controlled (which was not performed in our previous study on rat ventricular trabeculae; Fukuda et al., 2000), because the compound has been reported to specifically increase the affinity for Ca^{2+} of the low-affinity site of TnC (see Hagemeijer, 1993 and references therein).

Pimobendan (2×10^{-4} M) shifted the force–pCa curve leftward to a magnitude similar to that by MgADP or sTn reconstitution at SL 1.9 µm (i.e., $\sim$0.2 pCa units; see Fig. 2), with no effect on passive force (Fig. 6 A). However, unlike MgADP or sTn reconstitution, pimobendan exerted no effect on ΔpCa_{50} (see Fukuda et al., 2000). The Ca^{2+}-sensitizing effect of pimobendan was markedly diminished after sTn reconstitution, with no significant increase in Ca^{2+} sensitivity of force at either SL (Fig. 6 B). Likewise, pimobendan did not affect the rate of rise of active force in control or sTn-reconstituted PLV (Fig. 6 C).

The values of pCa_{50}, n_H, and maximal force obtained with and without pimobendan are summarized in Table II.

Simulation of length-dependent activation

Finally, we analyzed the experimental findings based on a mathematical model (Ishiwata and Oosawa, 1974; Shimamoto et al., 2007; refer to Materials and methods and supplemental material for details). In this model, active isometric force is given by the interaction probability between the thick and thin filaments, and the probability depends on two factors: (1) Ca^{2+} concentration and (2) interfilament lattice spacing (Fig. S1). The equilibrium of the thin filament state between "off" and "on" (see Solaro and Rarick, 1998 and references therein) was assumed to change with the Ca^{2+} concentration based on the Hill equation, and expressed as lateral fluctuation in the myofilament lattice (Figs. S1 and S2). We performed experiments within the SL range (i.e., 1.9–2.3 µm); the overlap length between the thick and thin filaments is considered not to change significantly (see Moss and Fitzsimons, 2002 and references therein), but the lattice spacing does, due to titin extension, as revealed by previous studies with muscles expressing both N2B and N2BA titins (Fukuda et al., 2003), as in PLV (Terui et al., 2008).

Fig. 7 A shows the force–pCa curves simulated by our model for the experimental data with and without sTn reconstitution in PLV. The model parameters are n_{H_actin} and pCa_{50_actin}, representing the characteristics of thin filament on–off switching in response to Ca^{2+}. Based on Eq. 6, we simulated the force–pCa curves of PLV with and without sTn reconstitution, and thereby the pCa_{50} and ΔpCa_{50} values were calculated (for optimization of fitting, see supplemental material).

Under the control condition without sTn reconstitution, a reduction in the lattice spacing due to an increase

in SL from 1.9 to 2.3 µm (refer to Materials and methods) increased maximal Ca^{2+}-activated force and shifted the force–pCa curve leftward, resulting in ΔpCa_{50} of 0.24 pCa units. As shown in Fig. S2, an increase in n_{H_actin}
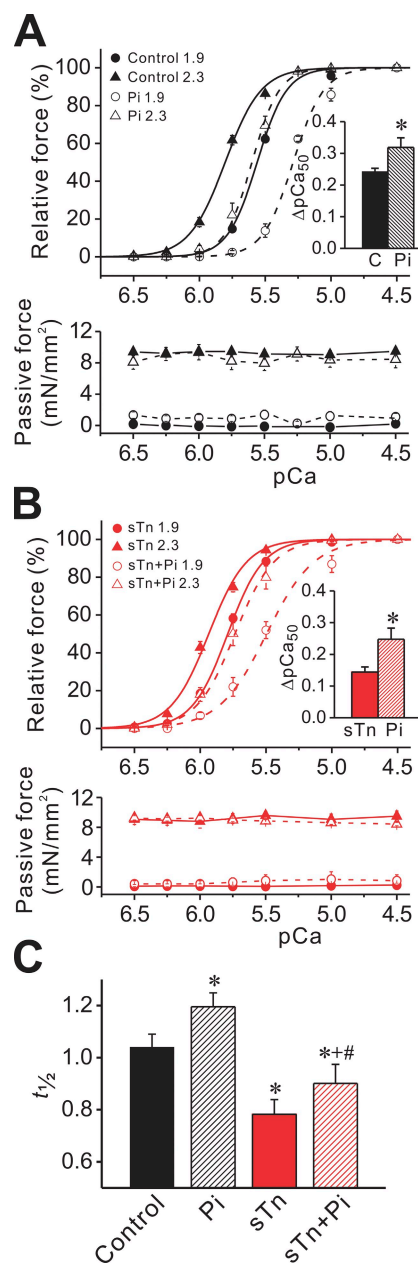

Figure 3. Effects of Pi on Ca^{2+} sensitivity of force and $t_{1/2}$ with and without sTn reconstitution. (A) Effect of 20 mM Pi on force–pCa curves (top) and passive force (bottom) in control PLV. Solid lines, −Pi; dashed lines, +Pi. (Inset) Comparison of ΔpCa_{50} in the absence and presence of Pi. *, P < 0.05. (B) Same as in A, but thin filaments were reconstituted with sTn. Solid lines, −Pi; dashed lines, +Pi. (Inset) Comparison of ΔpCa_{50} in the absence and presence of Pi. "sTn" indicates sTn-reconstituted PLV without Pi. *, P < 0.05. (C) Comparison of $t_{1/2}$ in control and sTn-reconstituted muscles in the absence and presence of 20 mM Pi. *, P < 0.05 compared with control; #, P < 0.05 compared with sTn; +, P < 0.05 compared with Pi. n = 6–7. Note that in A–C, data without Pi are the same as in Fig. 2.

decreased ΔpCa_{50} and concomitantly shifted the midpoint of the force–pCa curve rightward. On the other hand, an increase in pCa_{50_actin} linearly shifted the force–pCa curve leftward. To reproduce the experimental data after sTn reconstitution, we increased both n_{H_actin} and pCa_{50_actin}; as a result, the attenuation of length-dependent activation was well simulated, accompanied by appropriate pCa_{50} values for both SLs (as in Fig. 7 A; compare Figs. 2 and 3, and Terui et al., 2008).

Finally, we systematically investigated how varying the values of n_{H_actin} and pCa_{50_actin} affects length-dependent activation by constructing a 3-D graph consisting of n_{H_actin}, pCa_{50_actin}, and ΔpCa_{50} (Fig. 7 B). We found that ΔpCa_{50} was strongly influenced by n_{H_actin}; however, the contribution of pCa_{50_actin} to ΔpCa_{50} was minimal throughout the range we examined (see also Fig. S3). We plotted the pairs of the values of n_{H_actin} and pCa_{50_actin} that fulfill the linear relationship between pCa_{50} and ΔpCa_{50} (i.e., red points in Fig. 7 B), which was experimentally obtained in Fig. 4 A.

DISCUSSION

We demonstrated in this study that the Frank-Starling relation is strongly influenced by thin filament cooperative activation. The SL-dependent increase in Ca^{2+} sensitivity of force was inversely related to the rate of rise of active force, suggesting that length-dependent activation is tuned via on–off switching of the thin filament state in cardiac muscle. Further, our model analysis

revealed that thin filament cooperative activation, but not the affinity for Ca^{2+}, determines the magnitude of length-dependent activation, coupled with lattice spacing modulation. Here, we discuss the present findings, focusing on the role of thin filament cooperative activation in the regulation of length-dependent activation in cardiac muscle.

As is well established, strongly bound cross-bridges cooperatively activate the thin filaments (e.g., Bremel and Weber, 1972), resulting in the promotion of actomyosin interaction (refer to Introduction). Previous studies showing that NEM-S1 increases the speed of contraction in skinned fibers (Swartz and Moss, 1992, 2001; Fitzsimons et al., 2001a,b) support the notion that strongly bound cross-bridges accelerate the recruitment of neighboring myosin to the thin filaments via enhanced thin filament cooperative activation. In the present study, MgADP decreased $t_{1/2}$ at low concentrations (1 and 3 mM) but increased it at a high concentration (10 mM), and Pi exerted apparently similar effects at low (1, 3, and 5 mM) and high (10 and 20 mM) concentrations (Fig. 1; see Kentish, 1986). However, the underlying molecular mechanisms for the modulation of $t_{1/2}$, i.e., the rate of rise of active force, should differ for MgADP and Pi. At low MgADP concentrations (e.g., 3 mM used in the present study), the actomyosin–ADP complex may exhibit its promoting effect on actomyosin interaction by enhancing thin filament cooperative activation, but at high MgADP concentrations, the presence of large fractions of the complex may cause deceleration of contraction due to its slow cycling rate, as demonstrated

TABLE I

Summary of the values of passive force, maximal active force, pCa_{50}, and n_H in PLV under various conditions

	SL	Passive force	Maximal force	pCa_{50}	ΔpCa_{50}	n_H
	μm	*mN/mm^2*	*mN/mm^2*			
Without sTn reconstitution						
Control	1.9	∼0	57.25 ± 2.29	5.56 ± 0.01		3.86 ± 0.13
	2.3	9.40 ± 0.50	73.79 ± 3.72	5.80 ± 0.01	0.24 ± 0.01	3.17 ± 0.24
+ADP	1.9	∼0	67.19 ± 1.39[a] (78.41 ± 2.97)	5.82 ± 0.01[b]		3.44 ± 0.10[b]
	2.3	8.10 ± 0.67	75.61 ± 2.64	5.93 ± 0.01[b]	0.10 ± 0.01[b]	3.06 ± 0.16
+Pi	1.9	∼0	21.66 ± 1.39[a,b] (44.58 ± 5.53)	5.29 ± 0.03[b]		3.74 ± 0.31
	2.3	9.84 ± 0.95	38.53 ± 2.48[b]	5.60 ± 0.03[b]	0.31 ± 0.02[b]	4.18 ± 0.33[b]
With sTn reconstitution						
Control	1.9	∼0	51.83 ± 1.84	5.79 ± 0.01[b]		3.20 ± 0.18[b]
	2.3	10.23 ± 0.82	58.76 ± 3.14[b]	5.93 ± 0.02[b]	0.14 ± 0.02[b]	3.00 ± 0.08
+ADP	1.9	∼0	44.75 ± 5.61 (48.07 ± 4.49)	5.94 ± 0.02[b,c]		3.38 ± 0.18
	2.3	8.16 ± 0.49	49.90 ± 4.76[b]	6.01 ± 0.02[b,c]	0.07 ± 0.01[b,c]	3.52 ± 0.19[c]
+Pi	1.9	∼0	22.36 ± 1.19[a,b,c] (57.17 ± 2.70)	5.50 ± 0.04[c]		2.39 ± 0.29[b,c]
	2.3	9.49 ± 0.13	44.96 ± 2.32[b]	5.74 ± 0.04[c]	0.24 ± 0.02[c]	2.93 ± 0.30

Data are for Figs. 2 and 3. Maximal force was obtained by activating muscle at pCa 4.5 before construction of the force–pCa curve at each SL (passive force was measured just before activation at pCa 4.5). Numbers in parentheses indicate maximal force values obtained before ADP or Pi application. Maximal force obtained before sTn reconstitution at SL 1.9 μm: 54.36 ± 2.80, 48.65 ± 3.66, and 61.35 ± 2.08 mN/mm^2 for the control, ADP-, and Pi-treated group, respectively (P > 0.05 compared with the value after sTn reconstitution).

[a]P < 0.05 compared with the prior value.

[b]P < 0.05 compared with the corresponding values in control group without sTn reconstitution.

[c]P < 0.05 compared with the corresponding values in control group with sTn reconstitution.

previously in experiments measuring the shortening of the velocity at zero load (e.g., Cooke and Pate, 1985; Metzger, 1996), despite the highly activated state of the thin filaments. On the other hand, the binding of Pi to the actomyosin complex is reportedly enhanced upon the increase in the strain of the complex (Webb et al., 1986; Metzger, 1996). Therefore, at low concentrations, Pi may preferentially bind to the slowly cycling actomyosin–ADP complex, resulting in an increase in the rate of rise of active force, as demonstrated previously in experiments measuring kinetics following flash photolysis (Lu et al., 1993; Araujo and Walker, 1996), the shortening of the velocity at zero load (Metzger, 1996) and the rate of force redevelopment (k_{tr}) (Tesi et al., 2000). However, at high concentrations (e.g., 20 mM used in the present study), Pi may decrease the fraction of the actomyosin–ADP complex to a level where neighboring myosin cannot be effectively recruited to actin, resulting

in a decrease in the rate of rise of active force. Therefore, although the alteration of $t_{1/2}$ includes processes other than thin filament cooperative activation, the present findings allow us to consider that it at least in part reflects a change in thin filament cooperative activation.

MgADP at 3 mM increased the rate of rise of active force and, concomitantly, left-shifted the force–pCa curve (Figs. 1 and 2). The magnitude of the change was similar to that observed upon sTn reconstitution (i.e., direct modulation of regulatory proteins to enhance thin filament cooperative activation; see Terui et al., 2008) for both $t_{1/2}$ and Ca^{2+} sensitivity of force (Fig. 2). These findings suggest that, albeit modulated via different pathways, i.e., either indirectly or directly, thin filament cooperative activation is enhanced by a similar magnitude with 3 mM MgADP and sTn reconstitution. Interestingly, 3 mM MgADP increased both Ca^{2+} sensitivity of force and the rate of rise of active force in sTn-reconstituted PLV, accompanied by a marked depression of length-dependent activation (Fig. 2). These additive effects of MgADP suggest that thin filament cooperative activation can be synergistically modulated via strong-binding cross-bridge formation and regulatory protein isoform switching. In contrast, 20 mM Pi exerted effects opposite to those of 3 mM MgADP, with and without sTn reconstitution, by decreasing Ca^{2+} sensitivity of force and slowing the rate of rise of active force (Fig. 3). Therefore,
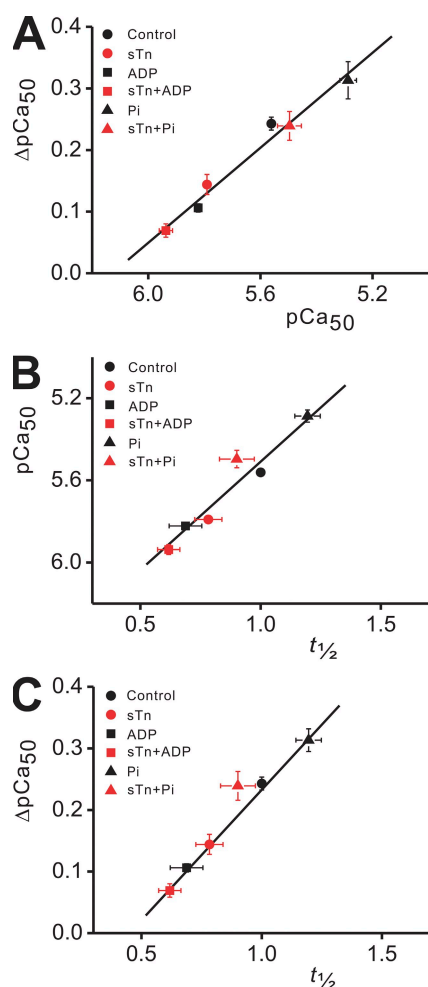

Figure 4. Linear regression analyses between $t_{1/2}$, pCa_{50}, and ΔpCa_{50}. The following relationships are shown: pCa_{50} versus ΔpCa_{50} (A, $R = 0.98$; $P < 0.0005$), $t_{1/2}$ versus pCa_{50} (B, $R = 0.96$; $P < 0.005$), and $t_{1/2}$ versus ΔpCa_{50} (C, $R = 0.97$; $P < 0.001$). Plots were constructed using the data in Figs. 2 and 3 (pCa_{50} obtained at SL 1.9 µm).
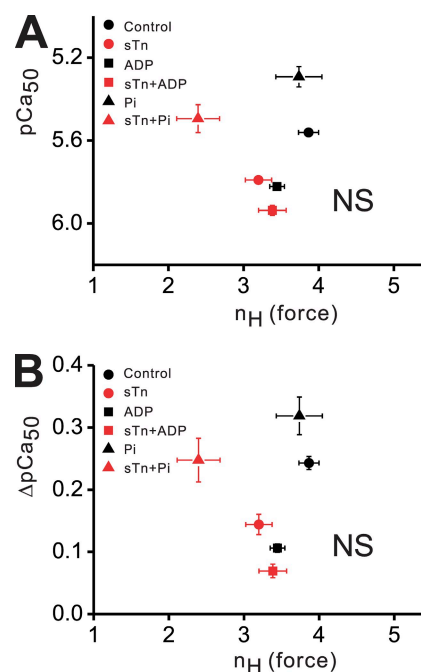

Figure 5. Relation between the n_H of the force–pCa curve (i.e., n_H [force]) and ΔpCa_{50} obtained experimentally under various conditions. (A) Plot of n_H (force) versus pCa_{50}. (B) Plot of n_H (force) versus ΔpCa_{50}. No significant correlation was found between the parameters in either graph (see Dobesh et al., 2002). For both A and B, the n_H values used were from the force–pCa curve at SL 1.9 µm in Figs. 2 and 3 (see Table I). NS, not significant.
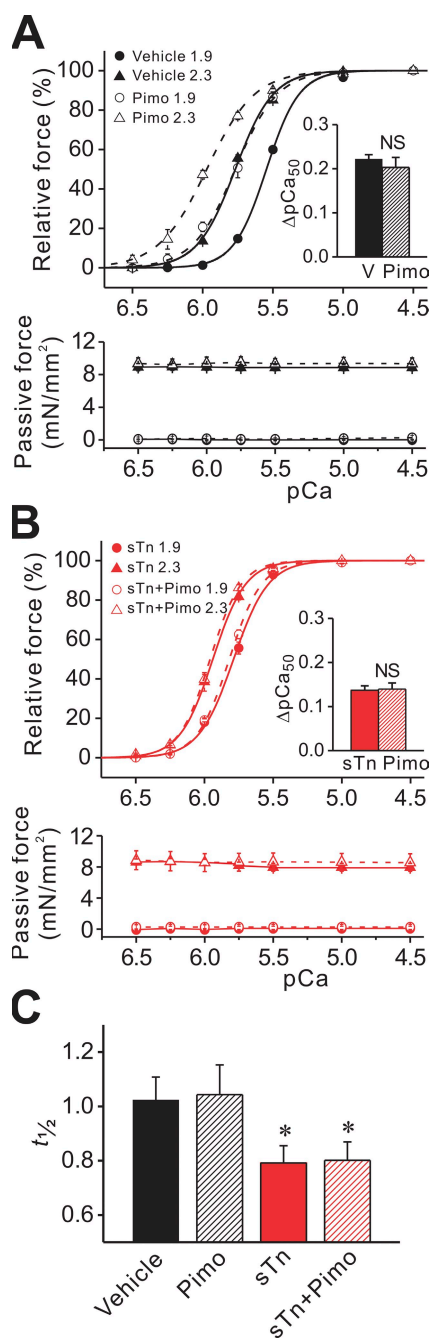
Figure 6. Effects of pimobendan on Ca^{2+} sensitivity of force and $t_{1/2}$ with and without sTn reconstitution. (A) Effect of 2×10^{-4} M pimobendan (Pimo) on force–pCa curves (top) and passive force (bottom) at SL 1.9 and 2.3 µm in control PLV. DMSO 1% was included in all solutions. Solid and dashed lines indicate in the absence and presence of pimobendan, respectively. (Inset) Comparison of ΔpCa_{50} in the absence and presence of pimobendan. V, vehicle without pimobendan. (B) Same as in A, but thin filaments were reconstituted with sTn. Solid and dashed lines indicate in the absence and presence of pimobendan, respectively. (Inset) Comparison of ΔpCa_{50} in the absence and presence of pimobendan. (C) Comparison of $t_{1/2}$ in control and sTn-reconstituted muscles in the absence and presence of 2×10^{-4} M pimobendan. *, P < 0.05 compared with vehicle. $n = 6$–7.

the observed effect of 20 mM Pi on length-dependent activation likely results from the reduced thin filament cooperative activation. Furthermore, pimobendan did not affect length-dependent activation, indicating that Ca^{2+} binding to TnC is not the parameter determining the magnitude of this phenomenon. Therefore, given the close relationship between $t_{1/2}$ (or pCa_{50}) and ΔpCa_{50} (Fig. 4), we consider that thin filament cooperative activation plays a pivotal role in setting the magnitude of length-dependent activation.

It has been reported in various experimental settings that a positive feedback mechanism exists between Ca^{2+} binding to TnC and cross-bridge formation in the sarcomere (Allen and Kurihara, 1982; Güth and Potter, 1987; Hoar et al., 1987; Hofmann and Fuchs, 1988; Zot and Potter, 1989). Therefore, the linear relationship of $t_{1/2}$ versus pCa_{50} observed in the present study (Fig. 4) likely reflects the positive feedback effect on Ca^{2+} binding to TnC via cross-bridge formation due to enhanced thin filament cooperative activation.

One may point out that k_{tr}, i.e., the sum of the apparent rate of cross-bridge attachment (f_{app}) and detachment (g_{app}) (Brenner, 1988; Swartz and Moss, 1992; Fitzsimons et al., 2001a,b, and references therein; Terui et al., 2008), more suitably represents thin filament cooperative activation in muscle mechanics than $t_{1/2}$. Indeed, k_{tr} is reportedly increased upon enhanced thin filament cooperative activation, when modulated directly (e.g., sTn reconstitution; Terui et al., 2008) or indirectly (NEM-S1 application; Swartz and Moss, 1992; Fitzsimons et al., 2001a,b). In the present study, 3 mM MgADP decreased k_{tr} at both maximal and submaximal activations (Fig. S4), in agreement with the result of previous studies with rabbit skeletal muscle (Lu et al., 1993; Tesi et al., 2000). MgADP is known to inhibit the release of ADP from the actomyosin complex at the end of the cross-bridge cycle (see Fukuda et al., 1998, 2000, and references therein). Therefore, the inhibitory effect of MgADP on g_{app} may overshadow its accelerating effect on cross-bridge formation (f_{app}), resulting in a decrease in k_{tr}. However, the observed increase in the rate of rise of active force, regardless of the Tn isoform, suggests that MgADP at low concentrations (such as 3 mM in the present experimental setting; see Figs. 1 and 2) accelerates f_{app} via enhancement of thin filament cooperative activation.

Pimobendan did not significantly increase Ca^{2+} sensitivity of force after sTn reconstitution in PLV (Fig. 6). It has, however, been reported that pimobendan increases Ca^{2+} sensitivity of force in amphibian skeletal muscles (Piazzesi et al., 1987; Wakisaka et al., 2000). The absence of Ca^{2+} sensitization observed in the present study may indicate the compound's specificity regarding the site of action; namely, in mammals, the binding affinity of pimobendan for (fast) skeletal TnC may be lower than that for cardiac TnC, producing a minimal effect on (fast) skeletal muscle. It should also be pointed out that

the rate of rise of active force was unaltered by pimobendan (Fig. 6), confirming our view that the increase in the rate of rise of active force by MgADP or sTn reconstitution results not from the increase in the affinity of TnC for Ca^{2+}, but from enhanced thin filament cooperative activation.

Dobesh et al. (2002) reported that the n_H of the force–pCa curve is not correlated with ΔpCa_{50}, leading them to conclude that thin filament cooperative activation plays no significant role in determining the magnitude of length-dependent activation. Consistent with this finding, we observed no significant correlation between the n_H of the force–pCa curve and ΔpCa_{50} (Fig. 5). However, it is unclear to what extent the steady-state n_H reflects thin filament cooperative activation. For instance, NEM-S1 or MgADP has been used to enhance thin filament cooperative activation; however, both NEM-S1 (Swartz and Moss, 1992, 2001; Fitzsimons and Moss, 1998; Fitzsimons et al., 2001a,b) and MgADP (at high concentrations: Fukuda et al., 1998, 2000) reportedly decrease the n_H of the force–pCa curve, resulting presumably from enhanced recruitment of neighboring cross-bridges, especially at low Ca^{2+} concentrations (see Fukuda et al., 1998 for ADP contraction occurring in the absence of Ca^{2+}). Therefore, in the present study, we regarded the rate of rise of active force as an index of thin filament cooperative activation (as in, e.g., Swartz and Moss, 1992, 2001; Fitzsimons et al., 2001a,b), rather than the n_H of the force–pCa curve.

Earlier, we discussed that at high activation states (i.e., high Ca^{2+} concentrations, MgADP application, or sTn reconstitution), cross-bridge recruitment upon SL elongation becomes less pronounced due to a decrease in the fraction of recruitable cross-bridges (that can potentially generate active force), resulting in the attenuation of length-dependent activation (see Fukuda et al., 2009

and references therein). The present model calculation provides a mechanistic insight into this interpretation. Namely, the SL elongation (i.e., lattice reduction) –induced increase in the probability of cross-bridge formation becomes less pronounced upon the increase in thin filament cooperative activation. This is because the acceleration of Ca^{2+}-dependent widening of the Gaussian distribution, of which the magnitude depends on n_{H_actin} (see Eq. 6 and Fig. S1), diminishes the lattice spacing–dependent change of the actomyosin interaction (determined by $d-a$). On the other hand, pCa_{50_actin} had little effect on the lattice spacing dependence; i.e., length-dependent activation. Indeed, the attenuation of length-dependent activation upon sTn reconstitution was quantitatively simulated by our model (Fig. 7 A) by increasing n_{H_actin} with appropriate pCa_{50} values for both short and long SLs as a result of an increase in pCa_{50_actin}. In addition, our model could quantitatively simulate the relationship of SL versus active force at various Ca^{2+} concentrations, converted from the force–pCa curves obtained under the control condition in Figs. 2 and 3 (i.e., shallower at high Ca^{2+} concentrations; Kentish et al., 1986; Fukuda et al., 2001b; see Fig. S5), emphasizing the adequacy of our model to analyze the molecular mechanism of length-dependent activation.

However, it is important to discuss limitations of the present study. First, we noted a mismatch between the experimental data and the simulated curves; namely, an increase in n_{H_actin} increased the steepness of the force–pCa curve at both SLs (compare Fig. 7 A), whereas the n_H of the force–pCa curve was not increased upon sTn reconstitution or MgADP application at either SL (Table I). We consider that this mismatch reflects the limitation of the experiments with skinned myocardial fibers. For example, internal sarcomere shortening that presumably occurs during isometric contraction (Fukuda et al., 2001b)

TABLE II

Summary of the values of passive force, maximal active force, pCa_{50}, and n_H in PLV with and without pimobendan

	SL	Passive force	Maximal force	pCa_{50}	ΔpCa_{50}	n_H
	μm	mN/mm^2	mN/mm^2			
Without sTn reconstitution						
Vehicle	1.9	~ 0	55.58 ± 3.97	5.55 ± 0.01		3.72 ± 0.14
	2.3	8.90 ± 0.52	76.68 ± 2.94	5.77 ± 0.01	0.22 ± 0.01	3.21 ± 0.04
+Pimobendan	1.9	~ 0	44.98 ± 3.76	5.77 ± 0.03^a		2.87 ± 0.13^a
	2.3	8.74 ± 1.04	61.81 ± 5.92	5.97 ± 0.02^a	0.20 ± 0.02	2.53 ± 0.25^a
With sTn reconstitution						
Vehicle	1.9	~ 0	53.68 ± 3.47	5.80 ± 0.01^a		3.29 ± 0.07^a
	2.3	8.88 ± 0.36	59.96 ± 3.15^a	5.93 ± 0.01^a	0.14 ± 0.01^a	3.45 ± 0.11
+Pimobendan	1.9	~ 0	51.52 ± 2.14	5.82 ± 0.01^a		3.68 ± 0.13
	2.3	9.37 ± 1.03	60.15 ± 3.55^a	5.96 ± 0.01^a	0.14 ± 0.01^a	3.82 ± 0.19^a

Data are for Fig. 6. Maximal force was obtained by activating muscle at pCa 4.5 before construction of the force–pCa curve at each SL (passive force was measured just before activation at pCa 4.5). Maximal force obtained before sTn reconstitution: 56.06 ± 3.42 and 54.25 ± 2.20 mN/mm^2 for vehicle and pimobendan-treated group, respectively (P > 0.05 compared with the value obtained after sTn reconstitution). Pimobendan did not significantly change maximal force (see Fukuda et al., 2000) with and without sTn reconstitution, and it did not change any parameter in sTn-reconstituted muscles.
[a]P < 0.05 compared with the corresponding values in the vehicle-treated group without sTn reconstitution.

may decrease active force production by a greater magnitude at high Ca^{2+} concentrations, resulting in an underestimation of the steepness of the force–pCa curve (as discussed in Fukuda et al., 2005). It should also be stressed that the mismatch reflects the limitation of the use of $t_{1/2}$ as an index of thin filament cooperative activation; namely, MgADP, Pi, or sTn reconstitution may alter the cross-bridge kinetics via a pathway that is not coupled with thin filament cooperative activation. Clearly, future studies with various techniques are needed to clarify this issue. Second, the decrease in the intermolecular distance, i.e., $d-a$ upon the addition of MgADP (earlier assumed to represent the lattice spacing modulation via cross-bridge formation in fast skeletal muscle; Shimamoto et al., 2007) enhanced length-dependent activation (Fig. S6) in contrast to the experimental result (Fig. 2). This apparent discrepancy may suggest that a change in thin filament cooperative activation has a greater impact on length-dependent activation, masking the effect of a cross-bridge–dependent lattice spacing change.

The 3-D graph obtained in the present model calculation (Fig. 7 B) suggests the role of the thin filaments in the regulation of length-dependent activation; namely, the magnitude of this phenomenon depends only slightly on the Ca^{2+}-binding ability of TnC, as confirmed by our

experimental analysis with pimobendan (Fig. 6 and Fukuda et al., 2000), but rather strongly on the cooperativity of the thin filament on–off switching (Figs. S1 and S2). Here, it is worthwhile noting that pCa_{50_actin} needed to be varied to quantitatively simulate the experimentally obtained relationship of pCa_{50} versus ΔpCa_{50} (Fig. 7 B). This may be due to a coupling between thin filament cooperative activation and cross-bridge formation, and to the ensuing feedback effect that enhances Ca^{2+} binding to TnC (Güth and Potter, 1987; Kurihara and Komukai, 1995). Therefore, the inverse relationship between pCa_{50} and ΔpCa_{50} (Fig. 4 A) may be an apparent phenomenon resulting from enhanced Ca^{2+} binding to TnC, coupled with acceleration of thin filament cooperative activation.

However, we admit that the present modeling is not suitable to account for the differing magnitudes of length-dependent activation in fast skeletal muscle versus slow skeletal muscle. Indeed, Konhilas et al. (2002a) reported that length-dependent activation is less in slow skeletal muscle, despite a lesser magnitude of thin filament cooperative activation. It is therefore likely that the difference in the magnitude of length-dependent activation between fast skeletal muscle and slow skeletal muscle results from factors that do not involve thin filament cooperative activation, such as isoform variance of
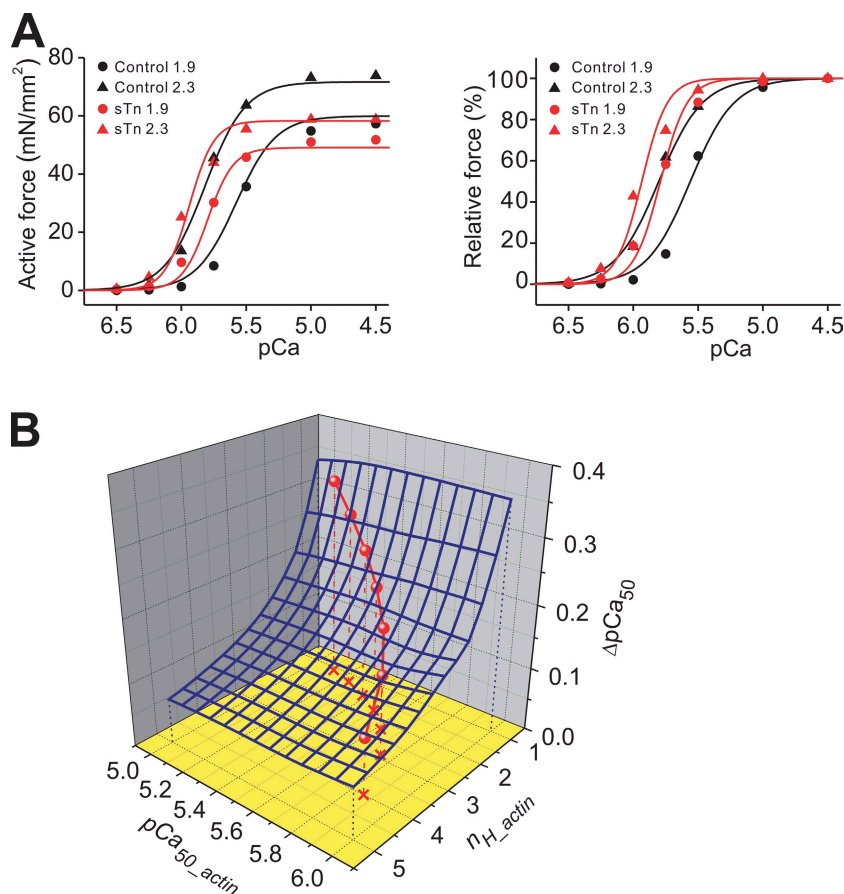

Figure 7. Simulation of active force development. (A) Force–pCa curves at SL 1.9 and 2.3 μm. (Left) Absolute data. (Right) Normalized data (normalized at pCa 4.5). Symbols are experimental data (the same as in Figs. 2 and 3; see Table I for absolute data). Error bars are not shown for simplicity. And solid lines are simulation results (black, control; red, sTn reconstitution). The differences between the values of the midpoint of the force–pCa curve at SL 1.9 and 2.3 μm are 0.24 and 0.14 pCa units in control and sTn-reconstituted PLV, respectively (see Table I). (B) 3-D graph showing the relationship between n_{H_actin}, pCa_{50_actin}, and ΔpCa_{50} obtained from the model analysis. Calculations were conducted at various values of n_{H_actin} per unit of 0.5 and pCa_{50_actin} per unit of 0.25, and, thereby, the ΔpCa_{50} values obtained from Eq. 6 (refer to Materials and methods) are plotted as the continuous mesh blue plane. Red points indicate the pairs of n_{H_actin} and pCa_{50_actin} that fulfill the linear relationship between pCa_{50} and ΔpCa_{50} (as in Fig. 4 A).

Terui et al. 479

thin filament– and thick filament–based proteins. It is an area of future research to clarify this issue by using various skeletal muscle tissues.

Considering that Ca^{2+} sensitivity of force varies depending on the type of heart disease (for review see Ohtsuki and Morimoto, 2008), it is likely that thin filament cooperative activation is altered in disease. The findings of the present study suggest that length-dependent activation is modulated via mutation occurring in the thin filaments and/or breakdown of ATP and the ensuing elevations in ADP and Pi in the vicinity of cross-bridges. Indeed, it has been reported that the Frank-Starling mechanism is depressed in skinned left ventricular muscles from patients with terminal heart failure (Schwinger et al., 1994; Brixius et al., 2003). It would be interesting to simulate, based on the 3-D state diagram (Fig. 7 B), how the Frank-Starling relation is altered by the occurrence of a mutation in a regulatory protein and/or the breakdown of ATP in various types of heart disease in various animal species, including humans.

In conclusion, thin filament cooperative activation plays a central role in the regulation of the Frank-Starling mechanism of the heart.

REFERENCES

Allen, D.G., and J.C. Kentish. 1985. The cellular basis of the length-tension relation in cardiac muscle. *J. Mol. Cell. Cardiol.* 17:821–840. doi:10.1016/S0022-2828(85)80097-3

Allen, D.G., and S. Kurihara. 1982. The effects of muscle length on intracellular calcium transients in mammalian cardiac muscle. *J. Physiol.* 327:79–94.

Araujo, A., and J.W. Walker. 1996. Phosphate release and force generation in cardiac myocytes investigated with caged phosphate and caged calcium. *Biophys. J.* 70:2316–2326. doi:10.1016/S0006-3495(96)79797-7

Arteaga, G.M., K.A. Palmiter, J.M. Leiden, and R.J. Solaro. 2000. Attenuation of length dependence of calcium activation in myofilaments of transgenic mouse hearts expressing slow skeletal troponin I. *J. Physiol.* 526:541–549. doi:10.1111/j.1469-7793.2000.t01-1-00541.x

Brandt, P.W., R.N. Cox, M. Kawai, and T. Robinson. 1982. Effect of cross-bridge kinetics on apparent Ca^{2+} sensitivity. *J. Gen. Physiol.* 79:997–1016. doi:10.1085/jgp.79.6.997

Brandt, P.W., M.S. Diamond, J.S. Rutchik, and F.H. Schachat. 1987. Co-operative interactions between troponin-tropomyosin units extend the length of the thin filament in skeletal muscle. *J. Mol. Biol.* 195:885–896. doi:10.1016/0022-2836(87)90492-X

Brandt, P.W., D. Roemer, and F.H. Schachat. 1990. Co-operative activation of skeletal muscle thin filaments by rigor crossbridges. The effect of troponin C extraction. *J. Mol. Biol.* 212:473–480. doi:10.1016/0022-2836(90)90326-H

Bremel, R.D., and A. Weber. 1972. Cooperation within actin filament in vertebrate skeletal muscle. *Nat. New Biol.* 238:97–101.

Bremel, R.D., J.M. Murray, and A. Weber. 1973. Manifestations of cooperative behavior in the regulated actin filament during actin-activated ATP hydrolysis in the presence of calcium. *Cold Spring Harb. Symp. Quant. Biol.* 37:267–275.

Brenner, B. 1988. Effect of Ca^{2+} on cross-bridge turnover kinetics in skinned single rabbit psoas fibers: implications for regulation of muscle contraction. *Proc. Natl. Acad. Sci. USA.* 85:3265–3269. doi:10.1073/pnas.85.9.3265

Brixius, K., P. Savidou-Zaroti, W. Bloch, and R.H. Schwinger. 2003. Reduced length-dependent cross-bridge recruitment in skinned fiber preparations of human failing myocardium. *Eur. J. Appl. Physiol.* 89:249–256. doi:10.1007/s00421-002-0782-2

Cazorla, O., Y. Wu, T.C. Irving, and H. Granzier. 2001. Titin-based modulation of calcium sensitivity of active tension in mouse skinned cardiac myocytes. *Circ. Res.* 88:1028–1035. doi:10.1161/hh1001.090876

Cooke, R., and E. Pate. 1985. The effects of ADP and phosphate on the contraction of muscle fibers. *Biophys. J.* 48:789–798. doi:10.1016/S0006-3495(85)83837-6

Dobesh, D.P., J.P. Konhilas, and P.P. de Tombe. 2002. Cooperative activation in cardiac muscle: impact of sarcomere length. *Am. J. Physiol. Heart Circ. Physiol.* 282:H1055–H1062.

Fabiato, A. 1988. Computer programs for calculating total from specified free or free from specified total ionic concentrations in aqueous solutions containing multiple metals and ligands. *Methods Enzymol.* 157:378–417. doi:10.1016/0076-6879(88)57093-3

Fitzsimons, D.P., and R.L. Moss. 1998. Strong binding of myosin modulates length-dependent Ca^{2+} activation of rat ventricular myocytes. *Circ. Res.* 83:602–607.

Fitzsimons, D.P., J.R. Patel, K.S. Campbell, and R.L. Moss. 2001a. Cooperative mechanisms in the activation dependence of the rate of force development in rabbit skinned skeletal muscle fibers. *J. Gen. Physiol.* 117:133–148. doi:10.1085/jgp.117.2.133

Fitzsimons, D.P., J.R. Patel, and R.L. Moss. 2001b. Cross-bridge interaction kinetics in rat myocardium are accelerated by strong binding of myosin to the thin filament. *J. Physiol.* 530:263–272. doi:10.1111/j.1469-7793.2001.0263l.x

Fuchs, F., and Y.P. Wang. 1996. Sarcomere length versus interfilament spacing as determinants of cardiac myofilament Ca^{2+} sensitivity and Ca^{2+} binding. *J. Mol. Cell. Cardiol.* 28:1375–1383. doi:10.1006/jmcc.1996.0129

Fukuda, N., H. Fujita, T. Fujita, and S. Ishiwata. 1998. Regulatory roles of MgADP and calcium in tension development of skinned cardiac muscle. *J. Muscle Res. Cell Motil.* 19:909–921. doi:10.1023/A:1005437517287

Fukuda, N., H. Kajiwara, S. Ishiwata, and S. Kurihara. 2000. Effects of MgADP on length dependence of tension generation in skinned rat cardiac muscle. *Circ. Res.* 86:E1–E6.

Fukuda, N., J. O-Uchi, D. Sasaki, H. Kajiwara, S. Ishiwata, and S. Kurihara. 2001a. Acidosis or inorganic phosphate enhances the length dependence of tension in rat skinned cardiac muscle. *J. Physiol.* 536:153–160. doi:10.1111/j.1469-7793.2001.00153.x

Fukuda, N., D. Sasaki, S. Ishiwata, and S. Kurihara. 2001b. Length dependence of tension generation in rat skinned cardiac muscle: role of titin in the Frank-Starling mechanism of the heart. *Circulation.* 104:1639–1645. doi:10.1161/hc3901.095898

Fukuda, N., Y. Wu, G. Farman, T.C. Irving, and H. Granzier. 2003. Titin isoform variance and length dependence of activation in skinned bovine cardiac muscle. *J. Physiol.* 553:147–154. doi:10.1113/jphysiol.2003.049759

Fukuda, N., Y. Wu, G. Farman, T.C. Irving, and H. Granzier. 2005. Titin-based modulation of active tension and interfilament lattice spacing in skinned rat cardiac muscle. *Pflugers Arch.* 449:449–457. doi:10.1007/s00424-004-1354-6

Fukuda, N., T. Terui, I. Ohtsuki, S. Ishiwata, and S. Kurihara. 2009. Titin and troponin: central players in the frank-starling mechanism of the heart. *Curr. Cardiol. Rev.* 5:119–124. doi:10.2174/157340309788166714

Güth, K., and J.D. Potter. 1987. Effect of rigor and cycling cross-bridges on the structure of troponin C and on the Ca^{2+} affinity of the Ca^{2+}-specific regulatory sites in skinned rabbit psoas fibers. *J. Biol. Chem.* 262:13627–13635.

Hagemeijer, F. 1993. Calcium sensitization with pimobendan: pharmacology, haemodynamic improvement, and sudden death in patients with chronic congestive heart failure. *Eur. Heart J.* 14:551–566.

Hanft, L.M., F.S. Korte, and K.S. McDonald. 2008. Cardiac function and modulation of sarcomeric function by length. *Cardiovasc. Res.* 77:627–636. doi:10.1093/cvr/cvm099

Hoar, P.E., C.W. Mahoney, and W.G. Kerrick. 1987. MgADP- increases maximum tension and Ca^{2+} sensitivity in skinned rabbit soleus fibers. *Pflugers Arch.* 410:30–36. doi:10.1007/BF00581892

Hofmann, P.A., and F. Fuchs. 1988. Bound calcium and force development in skinned cardiac muscle bundles: effect of sarcomere length. *J. Mol. Cell. Cardiol.* 20:667–677. doi:10.1016/S0022-2828(88)80012-9

Huxley, A.F. 1957. Muscle structure and theories of contraction. *Prog. Biophys. Biophys. Chem.* 7:255–318.

Ishiwata, S., and S. Fujime. 1972. Effect of calcium ions on the flexibility of reconstituted thin filaments of muscle studied by quasielastic scattering of laser light. *J. Mol. Biol.* 68:511–522. doi:10.1016/0022-2836(72)90103-9

Ishiwata, S., and F. Oosawa. 1974. A regulatory mechanism of muscle contraction based on the flexibility change of the thin filaments. *J. Mechanochem. Cell Motil.* 3:9–17.

Katz, A.M. 2002. Ernest Henry Starling, his predecessors, and the "Law of the Heart". *Circulation.* 106:2986–2992. doi:10.1161/01.CIR.0000040594.96123.55

Kentish, J.C. 1986. The effects of inorganic phosphate and creatine phosphate on force production in skinned muscles from rat ventricle. *J. Physiol.* 370:585–604.

Kentish, J.C., H.E. ter Keurs, L. Ricciardi, J.J. Bucx, and M.I. Noble. 1986. Comparison between the sarcomere length-force relations of intact and skinned trabeculae from rat right ventricle. Influence of calcium concentrations on these relations. *Circ. Res.* 58:755–768.

Konhilas, J.P., T.C. Irving, and P.P. de Tombe. 2002a. Length-dependent activation in three striated muscle types of the rat. *J. Physiol.* 544:225–236. doi:10.1113/jphysiol.2002.024505

Konhilas, J.P., T.C. Irving, and P.P. de Tombe. 2002b. Myofilament calcium sensitivity in skinned rat cardiac trabeculae: role of interfilament spacing. *Circ. Res.* 90:59–65. doi:10.1161/hh0102.102269

Kurihara, S., and K. Komukai. 1995. Tension-dependent changes of the intracellular Ca^{2+} transients in ferret ventricular muscles. *J. Physiol.* 489:617–625.

Lu, Z., R.L. Moss, and J.W. Walker. 1993. Tension transients initiated by photogeneration of MgADP in skinned skeletal muscle fibers. *J. Gen. Physiol.* 101:867–888. doi:10.1085/jgp.101.6.867

Matsuba, D., T. Terui, J. O-Uchi, H. Tanaka, T. Ojima, I. Ohtsuki, S. Ishiwata, S. Kurihara, and N. Fukuda. 2009. Protein kinase A–dependent modulation of Ca^{2+} sensitivity in cardiac and fast skeletal muscles after reconstitution with cardiac troponin. *J. Gen. Physiol.* 133:571–581. doi:10.1085/jgp.200910206

McDonald, K.S., and R.L. Moss. 1995. Osmotic compression of single cardiac myocytes eliminates the reduction in Ca^{2+} sensitivity of tension at short sarcomere length. *Circ. Res.* 77:199–205.

Metzger, J.M. 1996. Effects of phosphate and ADP on shortening velocity during maximal and submaximal calcium activation of the thin filament in skeletal muscle fibers. *Biophys. J.* 70:409–417. doi:10.1016/S0006-3495(96)79584-X

Moss, R.L., and D.P. Fitzsimons. 2002. Frank-Starling relationship: long on importance, short on mechanism. *Circ. Res.* 90:11–13.

Moss, R.L., G.G. Giulian, and M.L. Greaser. 1985. The effects of partial extraction of TnC upon the tension–pCa relationship in rabbit skinned skeletal muscle fibers. *J. Gen. Physiol.* 86:585–600. doi:10.1085/jgp.86.4.585

Ohtsuki, I., and S. Morimoto. 2008. Troponin: regulatory function and disorders. *Biochem. Biophys. Res. Commun.* 369:62–73. doi:10.1016/j.bbrc.2007.11.187

Piazzesi, G., I. Morano, and J.C. Rüegg. 1987. Effect of sulmazole and pimobendan on contractility of skinned fibres from frog skeletal muscle. *Arzneimittelforschung.* 37:1141–1143.

Schwinger, R.H., M. Böhm, A. Koch, U. Schmidt, I. Morano, H.J. Eissner, P. Überfuhr, B. Reichart, and E. Erdmann. 1994. The failing human heart is unable to use the Frank-Starling mechanism. *Circ. Res.* 74:959–969.

Shimamoto, Y., F. Kono, M. Suzuki, and S. Ishiwata. 2007. Nonlinear force-length relationship in the ADP-induced contraction of skeletal myofibrils. *Biophys. J.* 93:4330–4341. doi:10.1529/biophysj.107.110650

Shimizu, H., T. Fujita, and S. Ishiwata. 1992. Regulation of tension development by MgADP and Pi without Ca^{2+}. Role in spontaneous tension oscillation of skeletal muscle. *Biophys. J.* 61:1087–1098. doi:10.1016/S0006-3495(92)81918-5

Solaro, R.J., and H.M. Rarick. 1998. Troponin and tropomyosin: proteins that switch on and tune in the activity of cardiac myofilaments. *Circ. Res.* 83:471–480.

Sosa, H., D. Popp, G. Ouyang, and H.E. Huxley. 1994. Ultrastructure of skeletal muscle fibers studied by a plunge quick freezing method: myofilament lengths. *Biophys. J.* 67:283–292. doi:10.1016/S0006-3495(94)80479-5

Swartz, D.R., and R.L. Moss. 1992. Influence of a strong-binding myosin analogue on calcium-sensitive mechanical properties of skinned skeletal muscle fibers. *J. Biol. Chem.* 267:20497–20506.

Swartz, D.R., and R.L. Moss. 2001. Strong binding of myosin increases shortening velocity of rabbit skinned skeletal muscle fibres at low levels of $Ca(^{2+})$. *J. Physiol.* 533:357–365. doi:10.1111/j.1469-7793.2001.0357a.x

Tachampa, K., H. Wang, G.P. Farman, and P.P. de Tombe. 2007. Cardiac troponin I threonine 144: role in myofilament length dependent activation. *Circ. Res.* 101:1081–1083. doi:10.1161/CIRCRESAHA.107.165258

Terui, T., M. Sodnomtseren, D. Matsuba, J. Udaka, S. Ishiwata, I. Ohtsuki, S. Kurihara, and N. Fukuda. 2008. Troponin and titin coordinately regulate length-dependent activation in skinned porcine ventricular muscle. *J. Gen. Physiol.* 131:275–283. doi:10.1085/jgp.200709895

Tesi, C., F. Colomo, S. Nencini, N. Piroddi, and C. Poggesi. 2000. The effect of inorganic phosphate on force generation in single myofibrils from rabbit skeletal muscle. *Biophys. J.* 78:3081–3092. doi:10.1016/S0006-3495(00)76845-7

Udaka, J., S. Ohmori, T. Terui, I. Ohtsuki, S. Ishiwata, S. Kurihara, and N. Fukuda. 2008. Disuse-induced preferential loss of the giant protein titin depresses muscle performance via abnormal sarcomeric organization. *J. Gen. Physiol.* 131:33–41. doi:10.1085/jgp.200709888

Umazume, Y., and S. Fujime. 1975. Electro-optical property of extremely stretched skinned muscle fibers. *Biophys. J.* 15:163–180. doi:10.1016/S0006-3495(75)85799-7

Wakisaka, C., N. Kitamura, T. Ohta, T. Kai, Y. Nakazato, and S. Ito. 2000. Effects of pimobendan, a new cardiotonic agent, on contractile responses in single skeletal muscle fibres of the frog. *Fundam. Clin. Pharmacol.* 14:379–385. doi:10.1111/j.1472-8206.2000.tb00419.x

Webb, M.R., M.G. Hibberd, Y.E. Goldman, and D.R. Trentham. 1986. Oxygen exchange between Pi in the medium and water during ATP hydrolysis mediated by skinned fibers from rabbit skeletal muscle. Evidence for Pi binding to a force-generating state. *J. Biol. Chem.* 261:15557–15564.

Yanagida, T., M. Nakase, K. Nishiyama, and F. Oosawa. 1984. Direct observation of motion of single F-actin filaments in the presence of myosin. *Nature.* 307:58–60. doi:10.1038/307058a0

Yoshino, S., Y. Umazume, R. Natori, S. Fujime, and S. Chiba. 1978. Optical diffraction study of muscle fibers. II. Electro-optical properties of muscle fibers. *Biophys. Chem.* 8:317–326. doi:10.1016/0301-4622(78)80014-3

Zot, A.S., and J.D. Potter. 1989. Reciprocal coupling between troponin C and myosin crossbridge attachment. *Biochemistry.* 28:6751–6756. doi:10.1021/bi00442a031